2018 V52-CCA Shortrange Windscanner

Pedersen, Anders Tegtmeier

Publication date:
2020

Document Version
Publisher's PDF, also known as Version of record

Citation (APA):
Pedersen, A. T. (2020). *2018 V52-CCA Shortrange Windscanner*. DTU Wind Energy. DTU Wind Energy E No. 0198

DTU Wind Energy E-Report-0198

2018 V52-CCA Shortrange Windscanner

Anders Tegtmeier Pedersen

DTU Wind Energy
Department of Wind Energy

DTU Wind Energy, Risø Campus,
Technical University of Denmark, Roskilde, Denmark

June 2020

Author: Anders Tegtmeier Pedersen
Title:
2018 V52-CCA
Shortrange Windscanner
Department: DTU Wind Energy

DTU Wind Energy E-Report 0198
June 25, 2020

ISSN:978-87-93549-66-1
ISBN:978-87-93549-66-1

Abstract (max. 2000 char)

This report has been written as part of the DTU Wind Energy V52-CCA cross-departmental measurement campaign in the autumn of 2018. and it describes the experimental details concerning the Shortrange Windscanner measurements performed as part of the campaign. The goal of the measurements is to investigate the wake turbulence characteristics of the Vestas V52 test turbine located at DTU Risø campus.
Because scanning the full wake cross-section would be quite time consuming and would thus impede the aim of measuring the turbulence it was decided to instead scan along two orthogonal lines stretching about 120 m in the horizontal and 90 m in the vertical direction and crossing approximately 110 m East of the turbine. This meant that a scan rate for the full trajectory of about 1 Hz could be achieved while measuring 322 points along the path. As an extra feature an additional scan trajectory was designed with the purpose of capturing the wake from the Babylon or multirotor turbine in case of southwesterly winds. The raw measurement data were converted into three orthogonal wind velocity components (u,v,w) together with associated spatial and temporal coordinates and stored in a DTU Wind Energy database.
The report is organised in the following way that. First the Shortrange Windscanner system is presented and the most important aspects of it explained. Then the measurement setup geometry is described together with the scanning trajectories optimised for fast scanning of the turbine wake. Finally, the processing of the most important measurement outputs is described together with a description of how and where they can be accessed.

Contract no:

Project no:
CCA-V52

Sponsorship:
DTU Wind Energy

Cover:

Pages: 12
Tables: 7
Figures: 8
References: 7

Technical University of Denmark
Frederiksborgvej 399
4000 Roskilde
Denmark
Tel. +45 93510786
antp@dtu.dk
www.vindenergi.dk

Contents

1 Introduction

This document gives a brief description of the setup and measurements performed with the Shortrange WindScanner in connection with the CCA-V52 campaign at DTU Risø in the fall of 2018. The aim of the campaign is to characterise the wake turbulence of the Vestas V52 test turbine located at DTU Risø campus through scanning the wind field along two orthogonal lines (horiontal and vertical) about 110 m downwind from the turbine.

2 Description of experiment

2.1 The Shortrange WindScanner

The Shortrange Windscanner system consists of three individual CW lidar units denoted R2D1, R2D2, and R2D3, respectively. Each unit is equipped with a rotatable prism-pair making it possible to steer the beam to any desired located within a cone with an opening angle of ±60° from zenith of the instrument. A third degree of freedom is governed by the focus distance of the beam controlling the distance from the lidar to the volume of air being probed. A central control unit links the three lidars so that the laser beams can be steered in sync pointing toward the same point in space. The laser wavelength is 1565 nm and each unit can measure radial wind speeds of about ±45 m/s at a rate of up to approximately 400 Hz. Further descriptions of the Shortrange WindScanner can be found in references [1, 2, 3] and related literature.

An important parameter of a CW lidar is the measurement probe length (or probe volume[1]) often defined as the distance on either side of the focus point where the measurement sensitivity is reduced by a factor of 2. For a Gaussian beam this is known as the Rayleigh range which can be calculated as

$$z_{\mathrm{R}} = \frac{\lambda}{\pi}\frac{d^2}{\alpha_0^2}, \tag{1}$$

where λ is the laser wavelength, d is the focus distance, and α_0 is the radius of the beam at the focusing lens, [4]. α_0 depends among other things on the focus distance and it is also known that the orientation of the steering prisms affects it, but a reasonable approximation for the WindScanners is $\alpha_0 = 20$ mm.

2.2 Setup

The three Windscanner units were each installed approximately 73 m from the origo of the measurement coordinate system, here defined by the alignment ball (see Section 2.3) with an angular separation of around 120°. The alignment ball is located approximately 1.8 m above terrain. The elevation angles of the Windscanner unites were set to about 30° from horizontal measured with a digital level and their azimuths to point approximately toward the alignment ball. The misalignment between the bore point direction and the actual direction to the ball is established through the 'find the ball' alignment procedure, see Section 2.3. For reference of the measured winds is installed a sonic anemometer on a short mast close to the alignment ball. The UTM positions (Easting, Northing, and height above sea level [5]) of the individual instruments and turbines can be found in Table 1 and a graphical representation is given in Fig. 1. The lidars acquired data synchronously

[1] The lidar actually probes a volume of air defined by the laser beam, but because the transverse components of this are negligible compared to the longitudinal component the probe volume is essentially reduced to a length.

at a rate of 322 Hz and the centre of the probe volume moved through the scan pattern once per second.

	Easting [m]	Northing [m]	Height [m]	E. rel. origo [m]	N. rel. origo [m]	H. rel. origo [m]
R2D1	317588.4901	6174968.903	11.4303	-67.4989	27.8350	-2.1983
R2D2	317661.0418	6174867.276	12.7641	5.0528	-73.7920	-0.8645
R2D3	317719.7844	6174977.794	12.4733	63.7954	36.7260	-1.1553
Alignment ball	317655.989	6174941.068	13.6286	0	0	0
Sonic	317653.1248	6174939.153	21.8067	-2.8642	-1.9150	8.1781
V52 spinner	317552.8424	6174983.3460	54.0186	-103,1466	42,2780	40,3900
Babylon turbine	317504.2981	6174852.9220	-	-151.6909	-88.1460	-

Table 1: UTM positions of instruments measured with Leica Multistation [6].

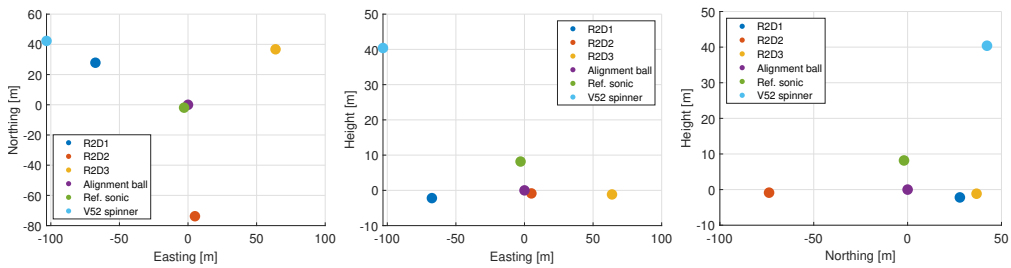

(a) Viewpoint: Above (b) Viewpoint: South (c) Viewpoint: East

Figure 1: UTM position of scanners, V52 spinner, alignment ball, and reference sonic seen from three different viewpoints. The alignment ball is placed approximately 1.8 m above terrain.

	Azimuth [°]	Elevation [°]
R2D1	0.4745	30.6100
R2D2	-0.7806	29.2771
R2D3	-1.3323	29.5639

Table 2: Scanner bore point directions. The azimuth here is the misalignment between the bore point azimuth and the direction to the alignment ball. The elevation is the elevation angle of the scanners measured from horizontal.

2.3 "Find the ball"

In order to find the pointing elevation and azimuth angles of each scanner the "Find the ball" procedure was applied.

A ball mounted on a rotating rig is placed near the common centre of the three scanner positions, and the prisms of each scanner is adjusted such that the laser beam hits the spinning ball; the rotation of the ball allows for the ball to be seen in the Doppler spectra. Once the beams are on the ball the focus motors are adjusted to give the highest backscatter signal in the Doppler spectra such that the beam waists coincide with the ball. The prism- and focus motor positions can finally be used to calculate the azimuth and elevation angles of the beams compared to the respective bore point directions.

2.4 Time of measurements

The campaign ran from 21st September 2018 to 30th October 2018 but not constantly. The measurements were periodically stopped to transfer data from the measurement computer or change scan pattern and also minor breakdowns of the WindScanner were experienced during the campaign. Table 3 gives an overview of when data was obtained together with the scan pattern used (see Sec. 3).

Start time	Stop time	Scan pattern
2018-09-21 12:30	2018-09-23 16:15	V52 narrow
2018-09-24 09:46	2018-09-25 08:46	V52 narrow
2018-09-25 12:46	2018-09-26 10:12	V52 narrow
2018-09-27 10:06	2018-10-01 09:00	V52 narrow
2018-10-01 11:33	2018-10-04 10:45	V52 narrow
2018-10-05 12:09	2018-10-08 08:32	V52 wide
2018-10-08 10:14	2018-10-08 13:52	Babylon
2018-10-09 10:42	2018-10-11 08:35	Babylon
2018-10-18 10:30	2018-10-23 06:23	V52 wide
2018-10-23 09:10	2018-10-24 04:50	V52 wide
2018-10-24 09:31	2018-10-26 12:21	V52 wide
2018-10-26 13:58	2018-10-30 09:28	V52 wide

Table 3: Time (UTC+1) of measurement and scan pattern used.

3 Scan patterns

Originally two scan patterns were designed and planned to be used depending on the wind direction; one to measure the wake behind the V52 turbine (westerly winds) and an other to measure the wake of the Babylon or multirotor turbine (southwesterly winds) [7]. Even for a scanning lidar, characterising the full rotor plane of either turbine is quite time consuming and thus counterproductive regarding the overall goal of measuring the turbulence profiles. Both patterns are therefore instead designed as a cross with a vertical part stretching about 90 m up from the origo (the alignment ball) and a horizontal part of the same length about 40 m above the ball and thus capturing the wind profile in two orthogonal lines exceeding the full span of the rotor plane. To minimise the time it takes to complete a full scan the beams will after completing the vertical scan move directly to the beginning of the horizontal part and vice versa so that the complete scan will look like a tilted bow tie figure. During the campaign it was decided to expand both these patterns to make them wider meaning that in total four scan patterns have been made, but because the narrow version of the Babylon pattern was never used only three patterns are described here.

The scan planes are defined as a vertical plane with the x-direction defining the normal to the plane, y is the horizontal in-plane component and z is the vertical in-plane component. The origo is defined to coincide with the alignment ball and the azimuth angle between x and East is $-22.3°$ for the V52 and $30.1°$ for the Babylon scan planes, respectively (see Figure 2).

In the following the scan trajectories as calculated from the actual lidar positions and orientations as well as the measured prism- and focus motor positions are presented. Shown is also tables stating the distance between the individual lidar unit and the points in the scan pattern closest and furthest away from it together with the associated probe lengths.

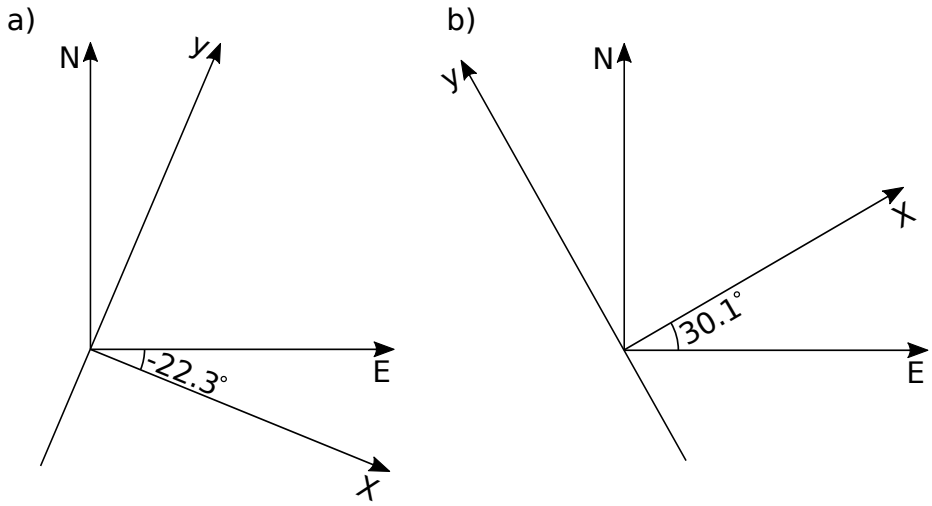

Figure 2: Definition of the scan planes with respect to East and North for the V52 (a) and the Babylon scan patterns (b). x defines the normal to scan plane which is consequently governed by the the yz plane.

3.1 V52 - narrow

Fig. 3 shows the average scan trajectory of the V52-narrow pattern in both UTM coordinates (*East,North,Height*) and in the scan plane (x, y, z). Average here means that it is the average of the positions of the three individual beam foci that is shown (the individual trajectories can be found in Appendix A). The tilted bow tie figure is clearly visible but seen is also that the measurement points do not lie in a perfect plane. However, this deviation from the ideal geometry is only about plus or minus 50 cm and small compared to the in-plane scale of the scan pattern.

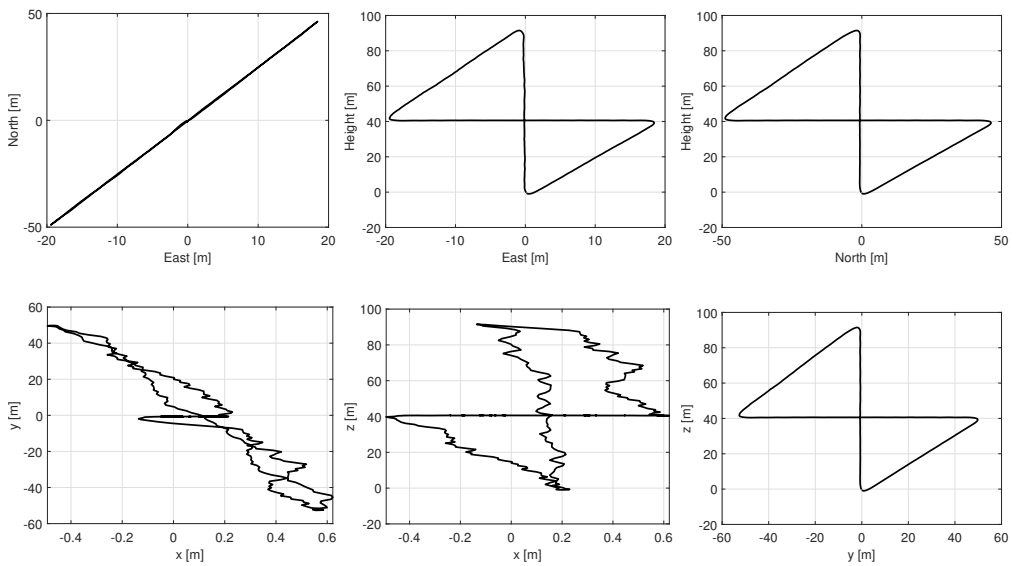

Figure 3: "V52-Narrow" scan trajectories relative to the origo in UTM coordinates (upper panel) and in the scan plane (lower panel).

Table 4 gives the maximum and minimum distances for each lidar unit to any point in the scan pattern together with the associated probe lengths defined as $2z_R$ (see Eq. (1)).

	Min. distance [m]	Max. distance [m]	Min. probe length [m]	Max. probe length [m]
R2D1	73.0	117.3	13.3	34.3
R2D2	55.0	127.4	7.5	40.4
R2D3	57.3	126.1	8.2	39.6

Table 4: Minimum and maximum distances to the V52 narrow scan pattern from each scanner and associated probe lengths.

3.2 V52 - wide

Fig. 4 shows the average scan trajectory of the V52-wide pattern in both UTM coordinates and in the scan plane and Table 5 shows the maximum and minimum distances and associated probe lengths for the V52. As can be seen the increase in width has led to an increase in the deviation from the ideal scan plane which has grown to about plus/minus 1 m.

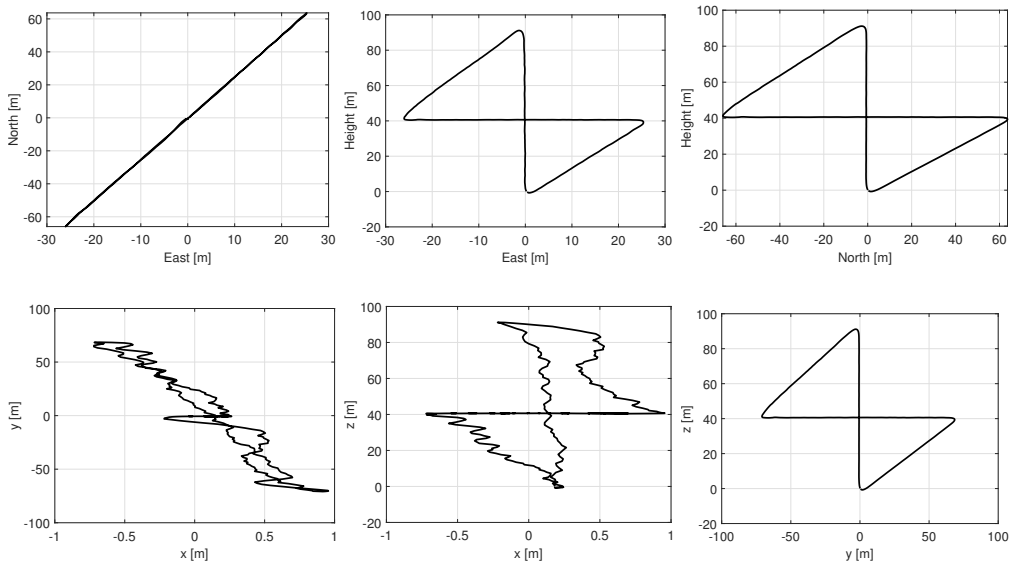

Figure 4: "V52-Wide" scan trajectories relative to the origo in UTM coordinates (upper panel) and in the scan plane (lower panel).

	Min. distance [m]	Max. distance [m]	Min. probe length [m]	Max. probe length [m]
R2D1	73.0	117.0	13.3	34.1
R2D2	52.5	145.0	6.9	52.4
R2D3	53.1	140.0	7.0	48.8

Table 5: Minimum and maximum distances to the V52 wide scan pattern from each scanner and associated probe lengths.

3.3 Babylon

Fig. 5 shows the average scan trajectory of the Babylon pattern in both UTM coordinates and in the scan plane and Table 6 shows the maximum and minimum distances and associated probe lengths for the V52.

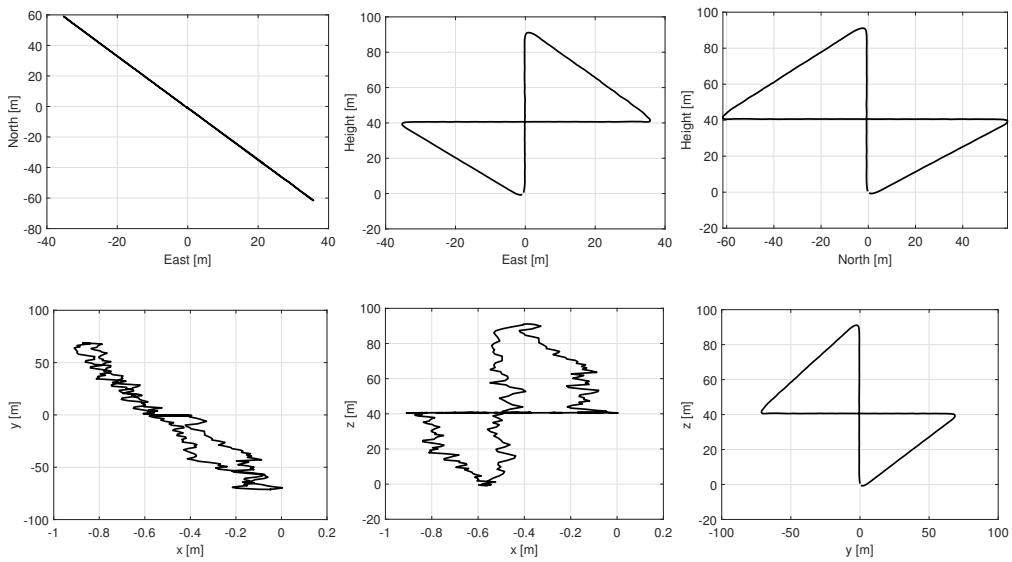

Figure 5: "Babylon" scan trajectories relative to the origo in UTM coordinates (upper panel) and in the scan plane (lower panel).

	Min. distance [m]	Max. distance [m]	Min. probe length [m]	Max. probe length [m]
R2D1	53.1	141.1	7.0	49.6
R2D2	52.6	145.1	6.9	52.4
R2D3	73.8	117.5	13.5	34.4

Table 6: Minimum and maximum distances to the Babylon scan pattern from each scanner and associated probe lengths.

4 Data processing

The raw measurement data obtained during the campaign in essence consist of prism- and focus motor positions together with the line-of-sight speeds from each unit and these have subsequently been processed into a more easily accessible format. The processed measurement data are stored in a database and a complete list of database entries can be found in Sec. 4.10. In the following some of the entries are explained in more detail.

4.1 u, v, and w

u, v, and w are the three wind velocity components defined as u pointing toward East, v toward North, and w vertically upwards and calculated via

$$\begin{aligned} u = &[V_1 (\alpha_2 \sin\phi_3 - \alpha_3 \sin\phi_2) + \\ &V_2 (\alpha_3 \sin\phi_1 - \alpha_1 \sin\phi_3) + \\ &V_3 (\alpha_1 \sin\phi_2 - \alpha_2 \sin\phi_1)] \,/\, (a \sin\phi_1 + b \sin\phi_2 + c \sin\phi_3)\,, \end{aligned} \tag{2}$$

$$\begin{aligned} v = &[V_1 (\beta_3 \sin\phi_2 - \beta_2 \sin\phi_3) + \\ &V_2 (\beta_1 \sin\phi_3 - \beta_3 \sin\phi_1) + \\ &V_3 (\beta_2 \sin\phi_1 - \beta_1 \sin\phi_2)] \,/\, (a \sin\phi_1 + b \sin\phi_2 + c \sin\phi_3)\,, \end{aligned} \tag{3}$$

$$w = [aV_1 + bV_2 + cV_3] \,/\, (a \sin\phi_1 + b \sin\phi_2 + c \sin\phi_3)\,, \tag{4}$$

where

$$\begin{aligned} \alpha_i &= \cos\theta_i \cos\phi_i, \\ \beta_i &= \sin\theta_i \cos\phi_i, \\ a &= \alpha_3\beta_2 - \alpha_2\beta_3, \\ b &= \alpha_1\beta_3 - \alpha_3\beta_1, \\ c &= \alpha_2\beta_1 - \alpha_1\beta_2. \end{aligned}$$

and V_{1-3} are the measured line-of-sight velocities, θ_{1-3} are the beam azimuth angles, and ϕ_{1-3} are the beam elevation angles (measured from horizontal) of the three lidar units and calculated from the motor positions.

4.2 2D u and v

During the campaign it was observed that at low measurement heights especially unit R2D3 was susceptible to erroneous measurement most likely due to the beam hitting a moving obstacle in the background. These errors lead to contamination of both u, v, and w, but with two correct line-of-sight measurements it is still possible to derive two of the three velocity components. Because w is less well-resolved at low heights anyway and because u and v are used in the calculation of the horizontal wind speed and direction it was decided to calculate and store a "2D" version of these.

The governing equations are a simplification of Eqs. (2) and (3)

$$u_{2D} = \frac{V_1 \cos\theta_2 \cos\phi_2 - V_2 \cos\theta_1 \cos\phi_1}{\cos\phi_1 \cos\phi_2 \sin(\theta_1 - \theta_2)}, \tag{5}$$

$$v_{2D} = \frac{V_2 \sin\theta_1 \cos\phi_1 - V_1 \sin\theta_2 \cos\phi_2}{\cos\phi_1 \cos\phi_2 \sin(\theta_1 - \theta_2)}. \tag{6}$$

There are three sets of (u_{2D}, v_{2D}) corresponding to the three combinations of lidars: $(1,2)$, $(2,3)$, and $(3,1)$ where the former is most likely to be free from erroneous estimates.

4.3 pos_id

As mentioned in Sec. 3 data is sampled at 322 Hz and one complete scan is 1 s meaning there are 322 measurement points distributed over the average scan pattern. These points are numbered $1 - 322$ beginning from the bottom of the scan pattern at the origo and each measurement is then labelled with a *pos_id* depending on which of the average scan

pattern points is closest to the actual measurement point. Notice that this is done for each of the three beam foci and because these do not coincide exactly in space they might not be labelled with the same *pos_id* (see also Appendix A). The latter is especially pronounced in the centre of the scan pattern where the vertical and horizontal scan lines cross.

4.4 sumofsep

The *Sum of Separation* is a measure of the separation in space between the foci of the three beams for each measurement. It is defined as the sum of the distances between each focus pair:

$$\begin{aligned}\text{sumofsep} =& \sqrt{(x_1 - x_2)^2 + (y_1 - y_2)^2 + (z_1 - z_2)^2} \\ &+ \sqrt{(x_2 - x_3)^2 + (y_2 - y_3)^2 + (z_2 - z_3)^2} \\ &+ \sqrt{(x_3 - x_1)^2 + (y_3 - y_1)^2 + (z_3 - z_1)^2}.\end{aligned} \tag{7}$$

4.5 vhorz

vhorz is the horizontal wind speed defined through.

$$\text{vhorz} = \sqrt{u^2 + v^2}. \tag{8}$$

Notice that it is the 3D u and v components that have been used and vhorz might therefore be contaminated at low heights (see Sec. 4.2).

4.6 dir

dir is the horizontal wind direction measured from North

$$\text{dir} = \arctan\left(\frac{v}{u}\right). \tag{9}$$

Again, it is the 3D u and v that have been used and *dir* might therefore be contaminated at low heights.

4.7 tilt

tilt is the vertical wind direction measured from horizontal:

$$\text{tilt} = \arctan\left(\frac{w}{u}\right). \tag{10}$$

4.8 vlos

vlos is the line-of-sight velocity measured by each lidar unit. It is defined as the 50% fractile of the thresholded Doppler spectrum.

4.9 Quality

quality is a measure of how representative the estimated line-of-sight velocity is of the probed wind. It is defined as the fraction of power in the Doppler peak contained within plus-minus one frequency bin of the bin nearest to the velocity estimation to the total spectrum power. This means that a very narrow Doppler peak will have a high *quality* (close to one) whereas a broad peak representing a very turbulent flow will have low quality. However, it also means that a weak signal spectrum containing perhaps only one spectral value will also have a high *quality* and *quality* is therefore a quantity that should be used with some caution and preferably in combination with *svmax* and *totalpower*.

4.10 Database

The measured and processed data is divided and stored in three similar tables according to the three scan patterns in the database: `ri-veadbs03.v52_cca_windscanner`
The three tables are named `v52_narrowscan`, `v52_widescan`, and `multirotor_widescan`, respectively. The data from the reference sonic can be found in the database `ri-veadbs04.v52_cca` in the columns labelled `v52_xx`.

Table 7 gives a complete list of the entries in the database together with their data format and a short description.

Name	Format	Description
Name	Char	Time of measurement 'YYYYMMDDHHmm'. Primary key
id	Int	Index of meas. within one minute (Name). Primary key
scan_id	Int	Index of completed scans within one minute (Name)
date_time	Datetime	Timestamp with ms precision. Based on datafile timestamps (UTC+1)
msinrun	Int	Milliseconds in run
sumofsep	Float	Sum of separations. Sum of the distances between the three beam foci
u	Float	Wind velocity u component. Along East
v	Float	Wind velocity v component. Along North
w	Float	Wind velocity w component. Along vertical
u2D{1-3, 1-3}	Float	u component derived from only two LOS measurements
v2D{1-3, 1-3}	Float	v component derived from only two LOS measurements
vhorz	Float	Horizontal wind speed
dir	Float	Horizontal wind direction
tilt	Float	Vertical wind direction
For each scanner:		
posid{1-3}	Int	Position index. Location of meas. point in scan pattern
ecoord{1-3}	Double	East coordinate for each laser beam
ncoord{1-3}	Double	North coordinate for each laser beam
hcoord{1-3}	Double	Height coordinate for each laser beam
vlos{1-3}	Float	Measured line-of-sight speed
svmax{1-3}	Float	Maximum spectral value in thresholded Doppler spectrum
totalpower{1-3}	Float	Total power in thresholded Doppler spectrum
quality{1-3}	Float	Quality of Vlos estimate

Table 7: Database entries.

A Individual scan trajectories

In reality the laser beam foci do not follow the exact same path through the scan pattern and the patterns presented in Sec. 3 are averages of the three beam paths. Below are shown the individual trajectories together with the average trajectory for comparison.

A.1 V52 - narrow

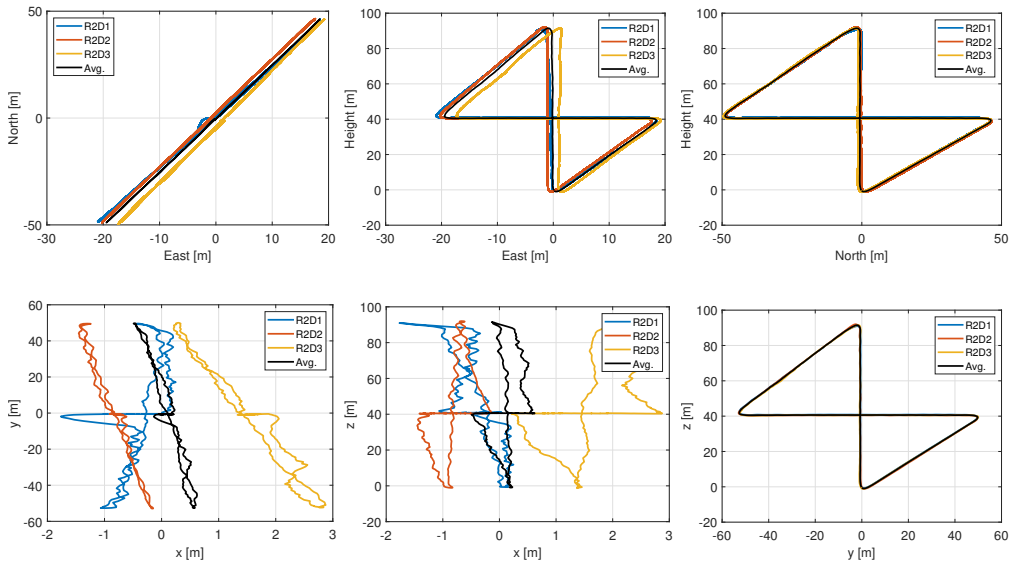

Figure 6: "V52 narrow" scan trajectories of the individual scanners relative to the origo in UTM coordinates (upper panel) and in the scan plane (lower panel).

A.2 V52 - wide

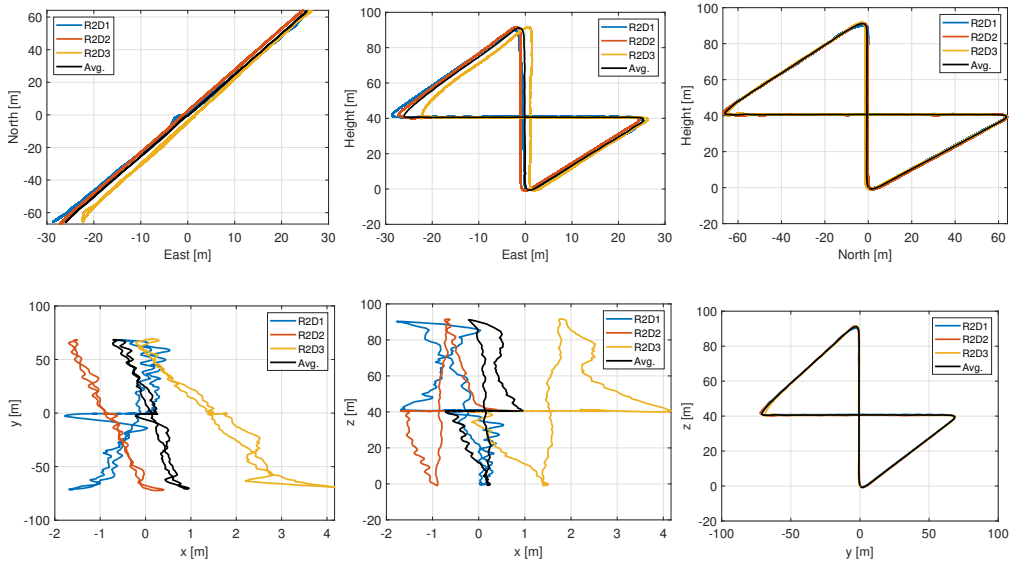

Figure 7: "V52 wide" scan trajectories of the individual scanners relative to the origo in UTM coordinates (upper panel) and in the scan plane (lower panel).

A.3 Babylon

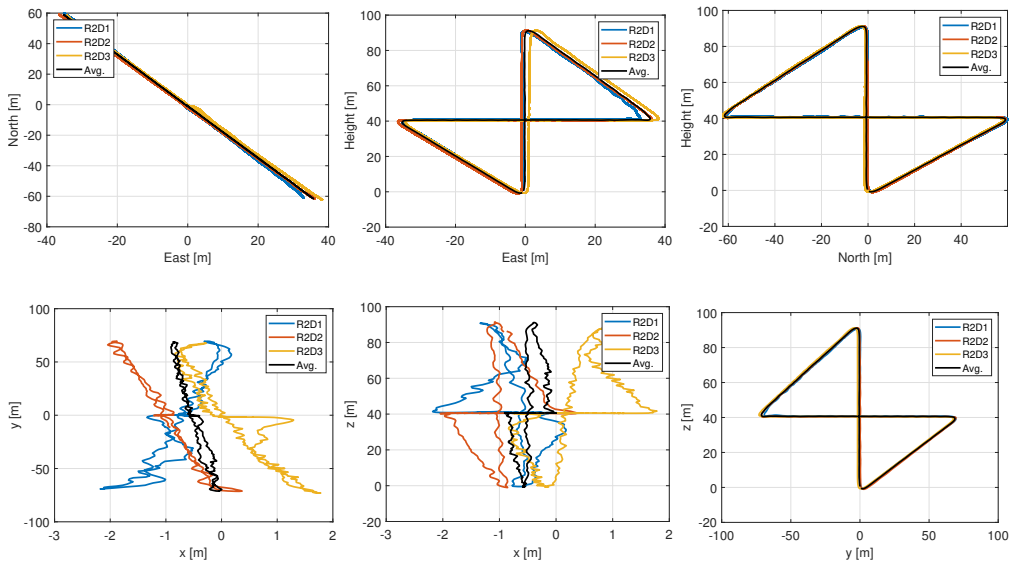

Figure 8: "Babylon" scan trajectories of the individual scanners relative to the origo in UTM coordinates (upper panel) and in the scan plane (lower panel).

References

[1] Nikola Vasiljevic, José M.L.M. Palma, Nikolas Angelou, José Carlos Matos, Robert Menke, Guillaume Lea, Jakob Mann, Michael Courtney, Luis Frölen Ribeiro, and Vitor M.M.G.C. Gomes. Perdigão 2015: Methodology for atmospheric multi-doppler lidar experiments. *Atmospheric Measurement Techniques*, 10(9):3463–3483, 2017.

[2] Eric Simley, Nikolas Angelou, Torben Krogh Mikkelsen, Mikael Sjöholm, Jakob Mann, and Lucy Y. Pao. Characterization of wind velocities in the upstream induction zone of a wind turbine using scanning continuous-wave lidars. *Journal of Renewable and Sustainable Energy*, 8(1), 2016.

[3] Nikolas Angelou, Farzad Foroughi Abari, Jakob Mann, Torben Mikkelsen, and Mikael Sjöholm. Challenges in noise removal from doppler spectra acquired by a continuous-wave lidar. In *Proceedings of the 26th International Laser Radar Conference*, 2012.

[4] Nikolas Angelou, Jakob Mann, Mikael Sjöholm, and Michael Courtney. Direct measurement of the spectral transfer function of a laser based anemometer. *Review of Scientific Instruments*, 83(3):033111, 2012.

[5] `https://en.wikipedia.org/wiki/Universal_Transverse_Mercator_coordinate_system`. Accessed: 2020-05-11.

[6] `https://leica-geosystems.com/products/total-stations/multistation/leica-nova-ms60`. Accessed: 2019-12-02.

[7] Paul van der Laan, Søren Juhl Andersen, Néstor Ramos García, Nikolas Angelou, Georg Pirrung, Søren Ott, Mikael Sjöholm, Kim Hylling Sørensen, Julio Xavier Vianna Neto, Mark C. Kelly, Torben Krogh Mikkelsen, and Gunner Chr. Larsen. Power curve and wake analyses of the vestas multi-rotor demonstrator. *Wind Energy Science*, 4(2):251–271, 2019.